Journal of Applied Electrochemistry **29**: 505–510, 1999.

Electrochemical nucleation of uranium in molten chlorides

K. SERRANO and P. TAXIL*
Laboratoire de Génie Chimique, U.M.R. 5503, 118 route de Narbonne, 31062 Toulouse Cedex 04, France
*(*author for correspondence)*

Received 20 March 1998; accepted in revised form 1 September 1998

Key words: chronoamperometry, electrocrystallization, molten chlorides, nucleation, uranium

Abstract

The electrochemical nucleation of uranium in molten salts on vitreous carbon was studied using chronoamperometry. It is shown that, whatever the applied overpotential and the temperature of the melt, the nucleation of uranium is instantaneous, three-dimensional and controlled by hemispherical diffusion. The diffusion coefficient of U^{III} is calculated. The value obtained by chronoamperometry is in good agreement with that obtained by cyclic voltammetry in previous studies [1].

List of symbols

A	nucleation rate constant per site (s^{-1})
C	bulk concentration of the electroactive species
$D_\times$	diffusion coefficient of the electroactive species $\times$ ($cm^2\ s^{-1}$)
F	Faraday constant (96 500 C mol^{-1})
I	current (mA)
M	molar weight (g mol^{-1})
n	number of exchanged electrons
N	density of nuclei created (cm^{-2})
N_0	total number of favorable sites (cm^{-2})
S	surface area of the working electrode (cm^2)

Greek symbols

ρ	density (g cm^{-3})

1. Introduction

It is now clearly established that uranium metal can be prepared by electrochemical reduction of UCl_3 in a NaCl–KCl mixture in a single step process [1]:

$$U^{III} + 3e^- \rightarrow U^0 \tag{1}$$

The objective of this work is to investigate the nucleation and crystal growth phenomena. For this purpose we use transient techniques at low concentrations of the electroactive species, whereas Martinot and Lopes [2]. chose steady state methods for the investigation of these phenomena for actinide and lanthanide electrodeposition. Our experimental results, obtained with chronoamperometry, are compared with the corresponding theoretical models [3–5]. The influence of the overpotential and the temperature on the nucleation mode is also considered.

2. Experimental process

Technical details on the cell used in this work can be found elsewhere [1, 6]. The melt was composed of an equimolar mixture of NaCl and KCl as solvent and U^{III} uranium ions as solute. The working and auxiliary electrodes were vitreous carbon rods (3 mm dia.). The surface area of the working and auxiliary electrodes were 1 cm^2 and 2 cm^2, respectively. The reference electrode was a 1 mm diameter platinum wire and its potential was fixed by the Pt(II)/Pt system [7].

The nucleation of uranium was demonstrated by cyclic voltammetry but the quantitative investigation of the process was performed by chronoamperometry on a vitreous carbon working electrode.

3. Results and discussion

3.1. *Cyclic voltammetry*

A typical cyclic voltammogram of NaCl–KCl–UCl_3(0.4 mass%) on a vitreous carbon electrode is shown in Figure 1. The cathodic part of this voltammogram presents a 'crossover' of the direct and the reverse scanning curve. The beginning of uranium metal formation, which is characterized by the rise in the cathodic current (Figure 1), is delayed. Indeed, a certain initiation overvoltage is required for the formation of the first nuclei of the new phase [8].

Furthermore, the reoxidation part exhibits a sharp decrease in current after the peak which is typical of a stripping effect due to the depletion of the metal deposited during the forward scan [9]. These features are characteristic of metal deposition associated with a nucleation process.

3.2. *Chronoamperometry*

Chronoamperometry is a method widely used to study nucleation phenomena in aqueous or molten media [6, 9–13]. Current transients for various potential pulses are shown in Figure 2. Their shape is associated with the nucleation and growth of a metal covering a foreign substrate [9]. The curves have three parts (I, II and III).

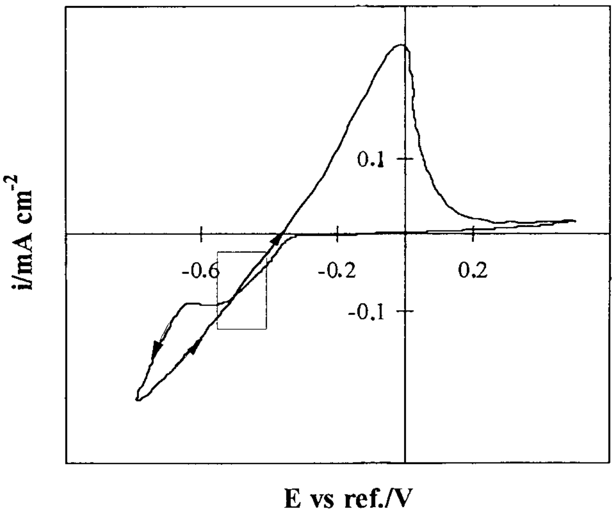

Fig. 1. Cyclic voltammogram illustrating the 'nucleation crossover effect' on the return sweep for deposition of uranium on vitreous carbon electrode with 0.4% mass of uranium; $\theta = 680\,°C$; scanning potential rate 200 mV s^{-1}.

The initial regime of each transient is characterised by a sharp decrease in current which corresponds, after charging of the double layer, to the formation of the first nuclei on the electrode (part I). This is followed by an increase in the current due to an increase in the electroactive area associated with crystal growth on the electrode (part II). This rise in current culminates in a broad maximum, I_m, the position of which on the time axis, t_m, depends upon the magnitude of the potential step. Finally, in part III, the slow decrease in current

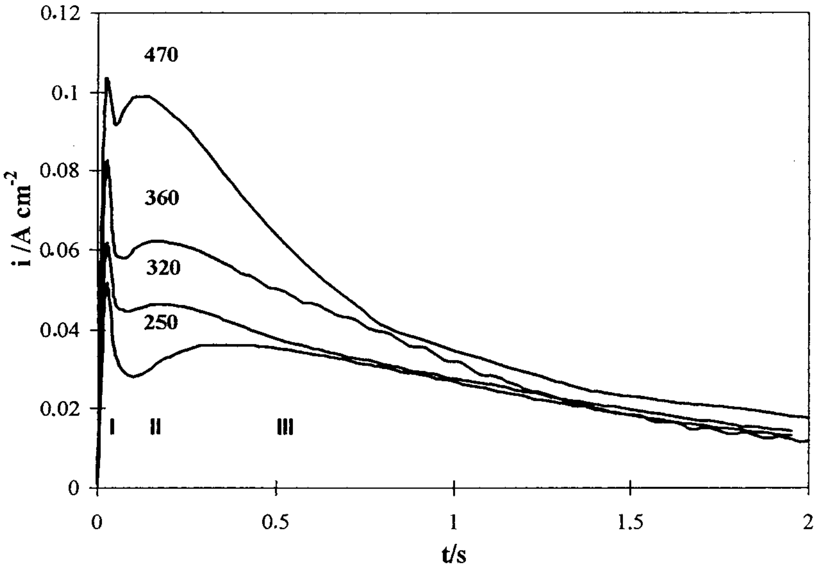

Fig. 2. Potentiostatic current–time transients of NaCl–KCl–UCl_3 at various cathodic overpotentials with 0.4% mass of uranium on a vitreous carbon cathode at 670 °C.

corresponds to the limitation of the reaction process by semi-infinite linear diffusion of the U(III) ions. The current time characteristic follows a linear relationship between I and $\sqrt{t}$ expressed by Cottrell's law [14].

The rising part (part II) of the chronoamperograms, characteristic of nucleation processes, was analysed and compared to models developed [5, 11] to describe two nucleation modes: (i) instantaneous nucleation in which all the uranium nuclei are created at the same moment at the beginning of the electrolysis; and (ii) progressive nucleation in which new crystals are continuously created throughout electrolysis.

According to [5, 11], the relationship between current, i, and time, t, at the beginning of the potential pulse, is given by an equation of the following type:

$$i = \alpha t^x \tag{2}$$

The exponent x depends on: (i) the type of nucleation (instantaneous or progressive), (ii) the geometry of the nuclei (e.g., hemisphere, cone, needle, disc), and (iii) the growth conditions (growth controlled by diffusion or by the kinetics of the electrochemical reaction). The various models, with corresponding values of α and x, were presented by Allongue et Souteyrand [11].

The best coincidence between our experimental data and the model in Equation 1 was obtained for $x = 1/2$. The proportionality between i and $t^{1/2}$ is shown in Figure 3 for various overvoltages. Thus, the nucleation is instantaneous, three-dimensional and the growth of the crystals is controlled by hemispherical or linear diffusion [11]. This conclusion is corroborated by scanning electron micrography of a covering of uranium on a vitreous carbon cathode after a short electrolysis time. In this micrograph (Figure 4), the size of the nuclei is uniform. They belong to a single generation of nuclei. Furthermore, it can be seen that the nuclei are hemispherical.

Scharifker and Hills [5]. developed nondimensional model adapted for this situation, that is, three-dimensional nucleation and diffusion controlled growth of crystals.

According to this model, with instantaneous nucleation, the ratio I/I_m is correlated to t/t_m by the following equation:

$$\left(\frac{I}{I_m}\right)^2 = \frac{1.9542}{t/t_m}\left\{1 - \exp\left(-1.2564\left(\frac{t}{t_m}\right)\right)\right\}^2 \tag{3}$$

where

$$t_m = \frac{1.2564}{N_0 \pi k D} \tag{4}$$

$$k = \left(\frac{8\pi C_0 M}{\rho}\right)^{1/2}$$

$$I_m = -0.6382\ nFDC_0S(kN_0)^{1/2} \tag{5}$$

and

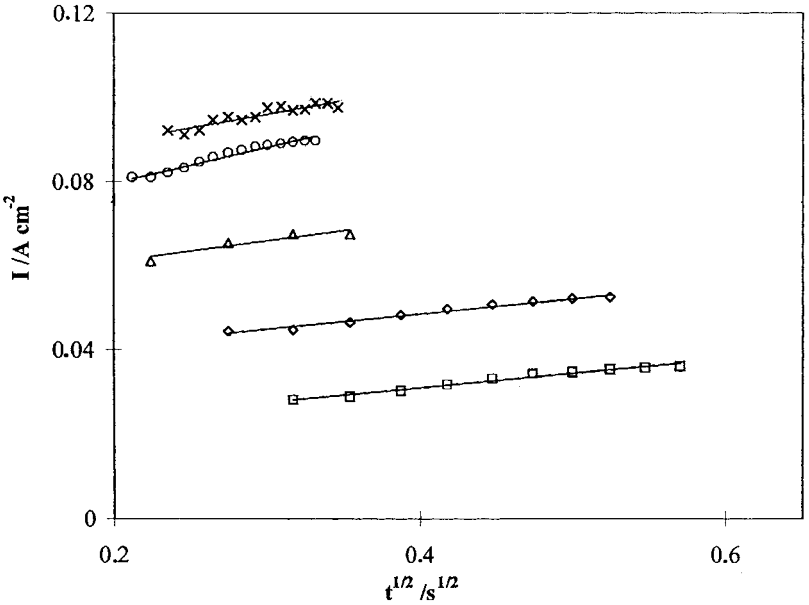

Fig. 3. Plots of $i/t^{1/2}$ constructed from the rising portion of the curves shown in Figure 2 at various overvoltages: (□) 250, (◇) 320, (△) 380, (○) 450 and (×) 470 mV.

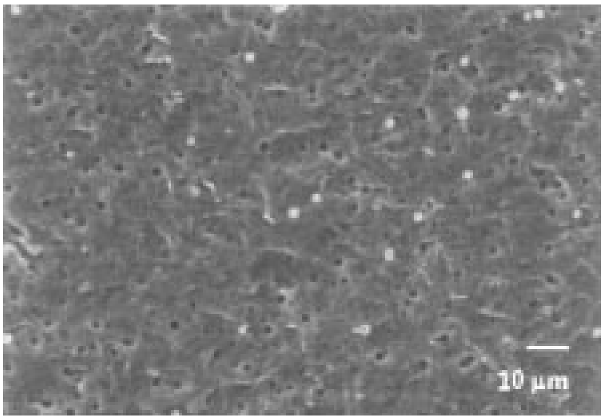

Fig. 4. Scanning electron micrograph (×680) of uranium deposit on vitreous carbon at 670 °C; $\eta = 320$ mV.

$$I_m^2 t_m = 0.1629\ (nFSC_0)^2 D \tag{6}$$

Adapted to progressive nucleation the equations are

$$\left(\frac{I}{I_m}\right)^2 = \frac{1.2254}{t/t_m}\left\{1 - \exp\left(-2.3367\left(\frac{t}{t_m}\right)^2\right)\right\}^2 \tag{7}$$

$$t_m = \left(\frac{4.6733}{AN_0\pi k'D}\right)^{1/2} \tag{8}$$

$$k' = \frac{4}{3}\left(\frac{8\pi C_0 M}{\rho}\right)$$

$$I_m = -0.4615\ nFSD^{3/4}C_0(k'AN_0)^{1/4} \tag{9}$$

and

$$I_m^2 t_m = 0.2598\ (nFSC_0)^2 D \tag{10}$$

Figure 5 allows the experimental curves $(I/I_m)^2 = (t/t_m)$ deduced from the chronoamperograms obtained at various overvoltages, to be compared to the theoretical curves corresponding to both modes of nucleation: Equations 3 and 7, respectively . The experimental data support Equation 3, that is, the instantaneous nucleation model, whatever the overvoltage. As shown in Figure 6, the experimental data always fit the model in the 670–715 °C temperature range. Thus, the nucleation mode of uranium is not influenced by temperature in this range.

Consequently, it can be concluded that nucleation of uranium follows the spontaneous nucleation model and crystal growth is limited by hemispherical diffusion whatever the overvoltage and the temperature of the melt.

Moreover, using the I_m and t_m values deduced from the chronoamperograms reported in Figure 2, the diffusion coefficient of the electroactive species can be calculated. According to Equation 6, the product $I_m^2 t_m$ is not expected to depend on the potential of the pulse. This is, indeed, verified experimentally, as shown in Table 1. Using the average value of $I_m^2 t_m$ (6×10^{-4} A^2 s cm^{-4}), we find

$$D_{U(III)} = 4.9 \times 10^{-5}\ \text{cm}^2\ \text{s}^{-1}$$

at 670 °C. This value is in good agreement with that obtained by cyclic voltammetry $D_{U(III)} = 4.4 \times 10^{-5}$ cm^2 s^{-1} at 670 °C) [1].

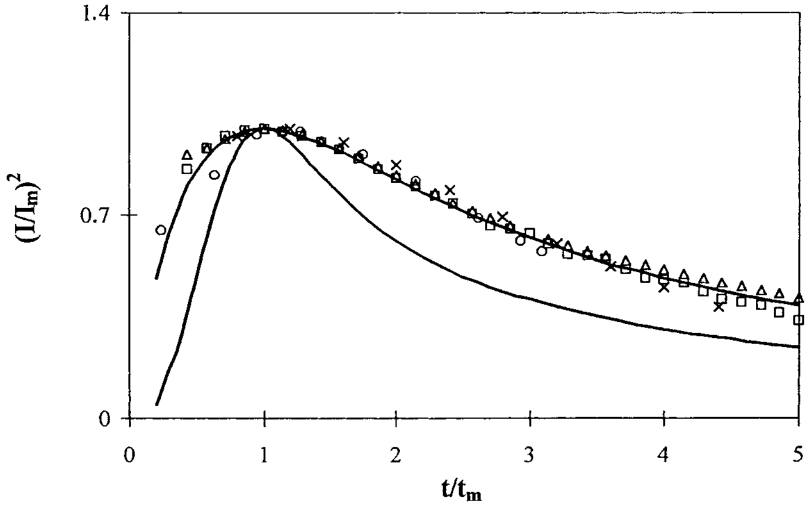

Fig. 5. Comparison of the dimensionless experimental data derived from the current–time transients with the theoretical models for instantaneous (i) and progressive nucleation (ii) at different overvoltages: (○) 250, (×) 300, (△) 320 and (□) 360 mV.

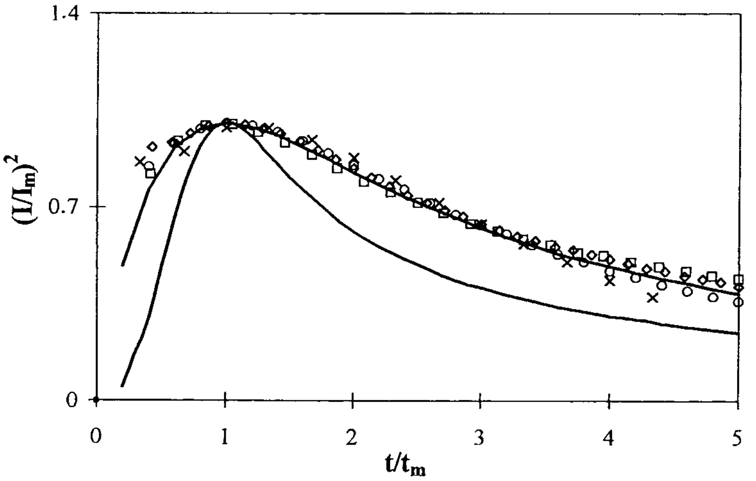

Fig. 6. Comparison of the dimensionless experimental data derived from the current–time transients with the theoretical models for instantaneous (i) and progressive nucleation (ii) at different temperatures: (×) 670, (○) 685, (□) 700 and (◇) 715 °C.

Table 1. Different values of $I_m^2 t_m$ with various overvoltages on vitreous carbon cathode

Overvoltage/mV	$10^4 I_m^2 t_m/\mathrm{A}^2\ \mathrm{s\ cm}^{-4}$
300	5.8
360	6.5
450	5.7
470	5.9
520	6.0

$\theta = 670\ ^\circ\mathrm{C}$ and $C_0 = 3 \times 10^{-5}\ \mathrm{mol\ cm}^{-3}$

3.3. *Determining the number of nuclei*

In the case of instantaneous nucleation and growth under hemispherical diffusion, the current transient obeys the following equation [11]:

$$i = \frac{-nF\pi(2C_0D)^{3/2}\sqrt{M}}{\rho^{1/2}} N t^{1/2} \qquad (10)$$

Equation 10 allows the number of nuclei for different overvoltages and temperatures to be calculated. Concerning the chronoamperograms obtained on vitreous carbon, Table 2 shows that the density of the nuclei increases significantly for increasing overvoltages. As expected, the number of nuclei increases significantly as the temperature increases (see Table 3).

Table 2. Influence of the overvoltage on the density of created nuclei

η/mV	$\alpha/\mathrm{mA\ s}^{-2}$	10^{-7} N/sites cm^{-2}
250	0.0683	3.6
320	0.1297	6.8
380	0.1418	7.4
450	0.1653	8.7

$C_0 = 3 \times 10^{-5}\ \mathrm{mol\ cm}^{-3}$; cathode: vitreous carbon, $\theta = 670\ ^\circ\mathrm{C}$

Table 3. Influence of the temperature on the density of created nuclei

T/°C	$\alpha/\mathrm{mA\ s}^{-2}$	10^{-6} N/sites cm^{-2}
670	0.2287	1.4
685	0.2447	1.5
700	0.3217	2.0
715	0.5319	3.3

$C_0 = 3 \times 10^{-5}\ \mathrm{mol\ cm}^{-3}$; $\eta = 180\ \mathrm{mV}$; cathode: vitreous carbon

4. Conclusion

It can be concluded that uranium nuclei are created instantaneously by the application of a potential pulse and that their growth is three-dimensional and limited by the diffusion of the uranium ions on an inert substrate; their shape is hemispherical. We have also highlighted that increase in both current density and temperature enhances the initial number of nuclei.

The literature [15–18] reports that uranium coatings in molten salts are very dendritic. If a smooth coating structure is required, experimental conditions must be adopted that favor the creation of a great number of nuclei and control the size of crystals. Thus the above conclusions are of great importance for the production of smooth coatings.

References

1. K. Serrano and P. Taxil, *J. Appl. Electrochem.* **29**(4) (1999) 497.
2. L. Martinot and L. Lopes, *Radiochim. Acta* **75** (1996) 105.
3. G. Gunawardena, G. Hills, I. Montenegro and B. Scharifker, *J. Electroanal. Chem.* **138** (1982) 225.
4. G. Hills and B.J. Scharifker, *J. Electroanal. Chem.* **130** (1981) 81.
5. B. Scharifker and G. Hills, *Electrochim. Acta* **28** (1983) 879.

6. P. Chamelot, B. Lafage and P. Taxil, *J. Electrochem. Soc.* **143** (1996) 1570.
7. R.J. Gale and D.G. Lovering, '*Molten Salt Techniques*' (Plenum Press, New York, 1984), p. 152.
8. B.N. Kabanov, '*Electrochemistry of Metals and Adsorption*', (Freund Publishing House, Israel, 1969), p. 3.
9. G.J. Hills, D.J. Schiffrin and J. Thomson, *Electrochim. Acta* **19** (1974) 657.
10. L. Legrand, A. Tranchart and R. Messina, *J. Electrochem. Soc.* **141** (1994) 378.
11. P. Allongue and E. Souteyrand, *J. Electrochem. Soc.* **139** (1992) 5.
12. X.H. Xu and C.L. Hussey, *J. Electrochem. Soc.* **139** (1992) 1295.
13. G.J. Hills, D.J. Schiffrin and J. Thomson, *Electrochim. Acta* **19** (1974) 671.
14. A.J. Bard and R.L. Faulkner, '*Electrochimie: Principes, Méthodes et Applications*' (Masson, Paris, 1983).
15. C. Marzano and R.A. Noland, Report A.N.L-5102 (1953).
16. G. Boisde, G. Chauvin, H. Coriou and J. Hure, *Electrochim. Acta* **5** (1961) 54.
17. M.B. Brodsky and B.G.F. Carleson, *J. Inorg. Nucl. Chem.* **24** (1962) 1675.
18. M. Kolodney, *J. Electrochem. Soc.* **129** (1982) 11.